



Publication Year	2017
Acceptance in OA @INAF	2023-01-20T11:13:43Z
Title	Processing tools refinement for the JIRAM arrival to Jupiter
Authors	Moriconi, Maria L.; NOSCHESE, RAFFAELLA; ADRIANI, Alberto
DOI	10.1140/epjp/i2017-11548-y
Handle	http://hdl.handle.net/20.500.12386/32944
Journal	THE EUROPEAN PHYSICAL JOURNAL PLUS
Number	132

Processing Tools Refinement in View of the JIRAM Arrival to Jupiter

Maria L. Moriconi², R. Noschese¹, A. Adriani¹

Maria L. Moriconi, ISAC-CNR, Via Fosso del Cavaliere, 100, 00133 Roma, Italy.
(m.moriconi@isac.cnr.it)

Raffaella Noschese, IAPS-INAF, Via Fosso del Cavaliere, 100, 00133 Roma, Italy.
(raffaella.noschese@iaps.inaf.it)

Alberto Adriani, IAPS-INAF, Via Fosso del Cavaliere, 100, 00133 Roma, Italy.
(alberto.adriani@iaps.inaf.it)

Corresponding author: Maria L. Moriconi, Institute of Atmospheric and Climatic Sciences -
CNR, Roma, Italy. (m.moriconi@isac.cnr.it)

¹Institute of Astrophysics and Space Planetology-INAF, Roma, Italy

² Institute of Atmospheric and Climatic Sciences - CNR, Roma, Italy.

Abstract

The JUNO mission, launched on August 2011 with the goal of investigating the origin and evolution of Jupiter, has been planned to reach Jupiter in July 2016. The months preceding the JUNO orbit insertion have been crucial for all the instrument teams to check the status and working abilities of the respective experiments. JIRAM (Jupiter Infrared Auroral Mapper), with its imager and slit spectrometer operating over the 2-5 μm spectral range [1] will attempt to reveal the deep atmospheric composition – 3 to 7 bars – in hot spots [2], to analyze the infrared auroral emissions of the H_3^+ molecules ionized by the Jovian magnetosphere currents and to detect the morphology and vertical structure of the clouds. Many different processing tools are in preparation to exploit the incoming JIRAM data. Here some results pertaining the image quality optimization and the visualizations that can be obtained from the spectrometer data management are reported.

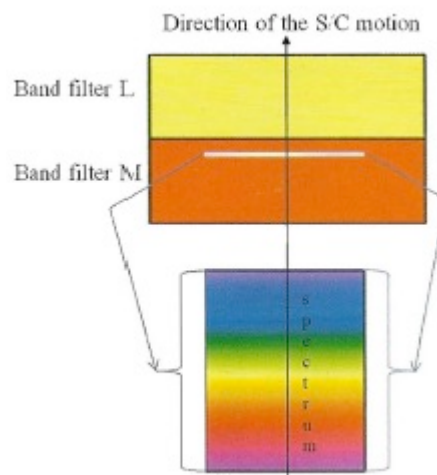
1. Introduction

JIRAM, onboard the Juno spacecraft, arrived at Jupiter on July 4 2016 with the goal to sound Jupiter's aurora and, more in general, the upper layers of the Jupiter's atmosphere [1]. JIRAM is essentially composed by a slit spectrometer and an imager, sharing the same telescope. The imager focal plane is in turn divided in two equal areas defined by the superimposition of two

35 different band-pass filters: filter L, centered at 3.45 μm with a 290 nm bandwidth, and filter M,
 36 centered at 4.78 μm with a 480 nm bandwidth. The spectrometer's slit is co-located in the M-
 37 filter imager's FOV (Figure 1).

38 The Juno spacecraft is planned to orbit 36 times along highly elliptical polar orbits. For each
 39 orbit the JIRAM observation period will be limited to a few hours before and after the perijove
 40 time. Indeed during the perijove pass the quality of the measurements could be strongly reduced
 41 and the focal planes could be at risk of damage by the environmental radiation (energetic
 42 electrons and protons) present in the Jupiter's magnetosphere. Therefore the extreme impact of
 43 the energetic particles will be prevented turning off the device during the mission phases where
 44 the spacecraft will cross the space regions at highest energetic particle density. Outside these
 45 regions the observations can be done according to the type of the planned observation. Auroral
 46 spectra and images are at higher risk of contamination for their low signal that requires long
 47 integration times up to the limit of the JIRAM capability. A custom denoising tool has been
 48 therefore implemented on the specific JIRAM demand. This tool takes advantage from the
 49 application of a contamination model on Jupiter sample images. This model predicts the noise on
 50 JIRAM focal planes by means a custom GEANT4 software application, based on the estimates of
 51 the "raw" external Juno radiation environment from the Divine/GIRE family of Jovian radiation
 52 models [3-5]; <http://www.openchannelfoundation.org/projects/GIRE/>). A description of the
 53 techniques setup to reduce the noise by environmental radiation on the JIRAM imagery is given
 54 in section 2 and a preview of the visualization tools assortment organized at today is presented in
 55 section 3. In section 4 a summary of the state of art and the works in progress are reported.

56



57

58

59

60

Figure 1 – Sketch of the optical arrangement of the two JIRAM's focal planes.

61

62

63

2. Noise reduction

64 Denoising is a reconstruction process in images that is intended to remove values that represent
 65 the noise or "foreign objects", or those artifacts that are not part of the image and conceal the true
 66 signal. Traditional linear filtering techniques frequently tend to blur the original signal, while this
 67 secondary effect can be overcome by using nonlinear ones. One popular class of nonlinear

68 filtering techniques is based on the singular-value-decomposition (SVD) method [6]. As a digital
69 image can be represented by a matrix of values, a pixel in an image corresponds to an intensity
70 value in the matrix. The SVD method works by identifying noisy pixel values by the small
71 singular values of the whole matrix. Often these SVD based algorithms are applied to the whole
72 image in a single, compute-intensive step, and do not address the problem of distinguishing
73 between significant and non-significant singular values. An improvement to this situation can be
74 achieved working on a block-based technique. More in detail a “neighborhood mask”, also
75 known as kernel, can be created, sliding across the input image at each point. Our denoising tool,
76 customized on the JIRAM demand, merges these two techniques. In other words a 5x5 kernel is
77 used as “neighborhood mask” sliding across every point of the JIRAM data images. For each
78 position the array is eventually organized as a vector where the single elements of the kernel are
79 sorted for increasing data value. Then the 25th element of this vector is replaced by the median
80 value if it results greater than the small singular value identified as minimum threshold applying
81 the SVD method to the 5x5 array kernel. The same procedure is applied for every data pixel
82 sliding the kernel across the whole image. This procedure can be reiterated as long as the percent
83 error calculated from the pixel data of the de-noised respect to the not contaminated image
84 reaches a threshold value arbitrarily fixed or tends to an asymptotic value. For JIRAM data we
85 fixed for the percent error a value inside the -10%/10% interval.
86 To check the validity of the above mentioned tool a test has been carried out on two Jupiter
87 sample pictures, imaging respectively a planet disk and a North Pole aurora (Figure 2).
88 Both the pictures of Figure 2 have been rescaled to the dynamical range expected for the proper
89 half focal plane of the imager – M and L band in a and b panels of the figure.

91 *2.1. Noise detector from penetrating radiation*

92
93 As reported in the Introduction, a Geant4 simulation for the JIRAM instrument has been
94 performed to determine the penetration efficiencies of high energy electrons and protons. A
95 detailed description of the method is reported in Becker et al. (2017). Briefly, the 436×270
96 HgCdTe pixel array of the JIRAM detector is the target where the penetrating event rate of the
97 environment radiation is simulated in events s^{-1} units. The energy deposited in the active regions
98 of the HgCdTe pixels is analyzed and associated with the unique external electron (or proton)
99 responsible for the noise. The deposited energy is converted into signal electrons using an
100 ionization rate of 1.2 eV per electron-hole pair (Klein, 1968). The typical noise signal due to an
101 impacting electron is ~ 64 DN per pixel (camera gain = $173 e^-/DN$). Impacts typically affect only
102 1 to 2 adjacent pixels due the lack of pixel-to-pixel diffusion in the JIRAM focal plane array. The
103 method permits us to simulate the contamination produced by different levels of environmental
104 radiation on the Jupiter images in DN.

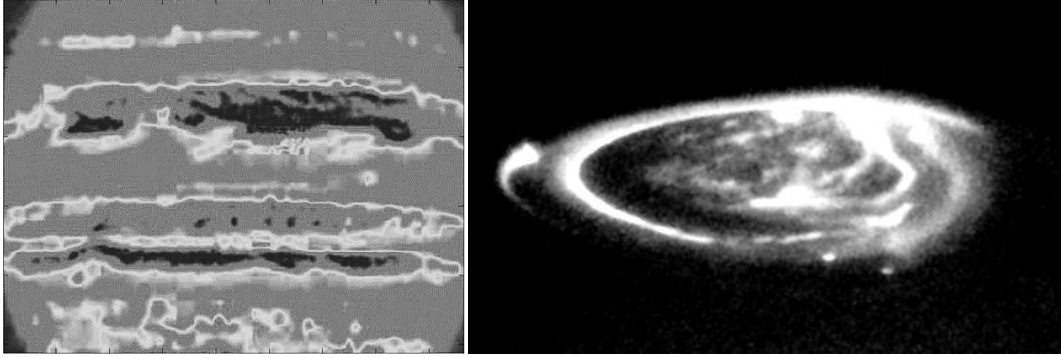


Figure 2 – Two sample pictures of Jupiter used to check the tolls for the noise reduction. Panel a: the planetary disk at 5 μm . Panel b: the North Pole aurora at UV wavelength.

2.2. *M band contamination and denoising*

The Jupiter disk image in M band, shown in Figure 2a, has been contaminated by means a simulated noise obtained from the combination of the measured dark current and the environmental radiation simulated as already described in section 1. The dark current values are those acquired during the Juno flyby at the Earth-Moon system and the radiation levels range from 10^3 and 10^4 $\text{e}^-/\text{cm}^2 \cdot \text{sec}$ for the M band dynamical range. In Figure 3a the picture of Figure 2a after the contamination is shown, along with the product of the application of three denoising tools: a Kuan filter, a Median filter and the denoising tool setup by the team where the Median filtering has been applied after the SVD analysis of the digital image.

Kuan filter is a minimum square error denoising technique built to improve images contaminated by random multiplicative noise. It is a linear filter which general form is

$$R(i,j) = \bar{I}(i,j) + [I(i,j) - \bar{I}(i,j) \times W(i,j)]$$

where (i,j) are the spatial coordinates of the current pixel, \bar{I} is the average of the pixels intensity in the moving window and W , characteristic for Kuan, is the weighting function ranging between 0 for flat regions and 1 for regions with high signal activity. The pixels to be filtered are replaced by the values calculated using the surrounding pixels.

Median filter is a nonlinear filtering method that replaces the original value of a pixel by the median of the pixels values in a specific neighborhood. Nonlinear filters derive from maximum likelihood estimation principle and assume the signal to be contaminated by additive noise Laplace distributed.

SVD+Median filter, already described at the beginning of this section, demonstrated the most efficient tool both in removing the simulated noise and to preserve the spatial feature edges in the image, as confirmed by a simple calculation of the percent error between the uncontaminated and filtered images whose vertical profile is reported in Figure 4.

2.3. L band contamination and denoising

140

141

142

143

144

145

146

147

148

149

150

151

152

153

154

155

156

157

158

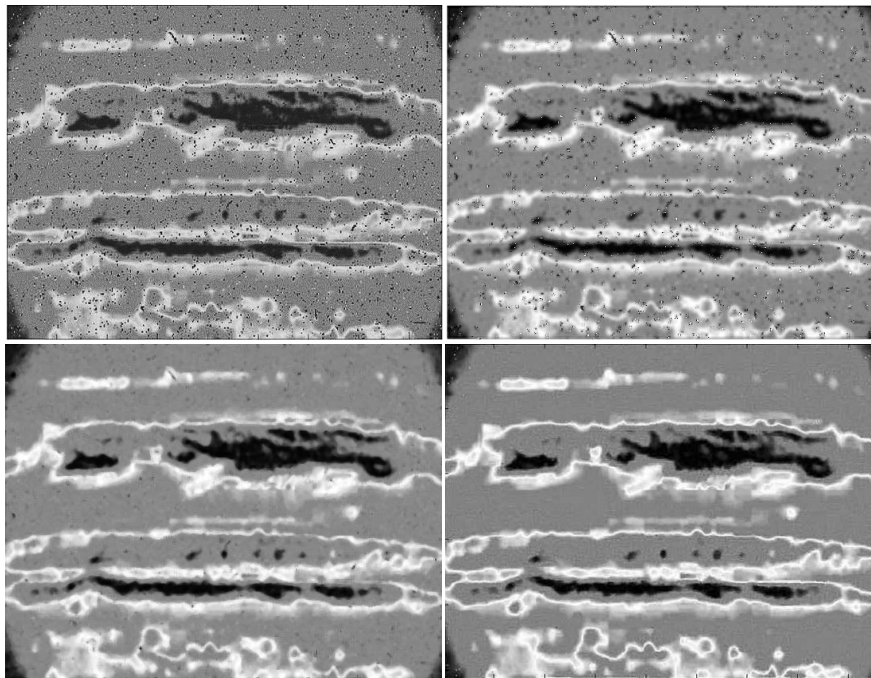
159

160

FUV imaging of the polar regions with the Space Telescope Imaging Spectrograph (STIS) - onboard the Hubble Space Telescope (HST) - provided a global view of the Jovian aurora with unprecedented spatial resolution. We have contaminated a STIS observations (Figure 2b) by the aforementioned JPL environmental radiation model and repeated the test already carried out for the M band case. As a very large digital matrix corresponds to this image, the noise matrix (432x256) it was necessary to replicate it, up to cover the whole image. This operation involved a periodicity in the noise structure, as shown in Figure 5a, conditioning the filtering result. However this is a false problem because this artifact will not be present in the real observations. In this case the maximum level of environmental radiation ($10^5 \text{ e}^-/\text{cm}^2 \cdot \text{sec}$) compatible with the JIRAM operative state has been applied to better simulate the more severe conditions that the instrument undergoes passing across the auroral precipitation lines during its polar perijove transit. In Figure 5 the contaminated STIS observation of Figure 2b is shown before and after the SVD+Median filtering. In this case the filtering was not be able to completely remove the noise, as in the M band case, however a satisfactory recover of the auroral spatial features has been reached. The percent error calculation (Figure 6) shows as the uncompleted noise removing exhibits strong oscillations around the central null value in correspondence of the bottom lines of the image, the noisiest in Figure 5b.

All the applied filtering refer to a 5x5 kernel.

161



162

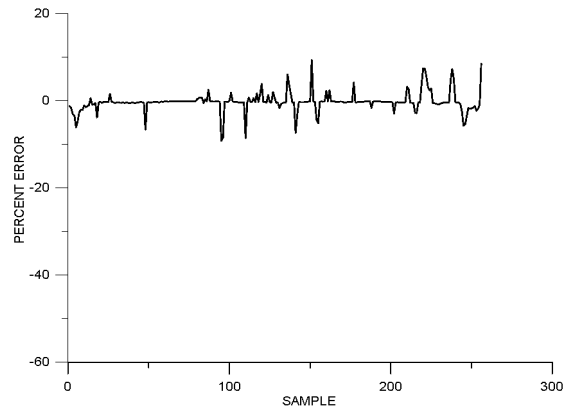
163

164

165

166

Figure 3 – The effect of the application of three denoising tools on the image of Figure 2a, artificially contaminated. Panel a: the contaminated image. Panel b: the same image after the Kuan filter application. Panel c: as before after the median filter application. Panel d: as before after the SVD+median filter application.



167

168

169

170

171

Figure 4 – The percent difference between the image of Figure 2a and Figure 3d. The plotted vertical profile refers to the sample crossing the center of the two images.

172

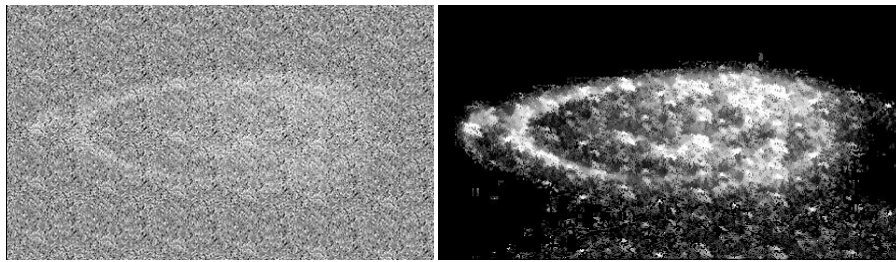
3. Visualizations from spectral data management

173

JIRAM can directly visualize the selected targets by means of its spectral imagers in L and M band, however it is possible also to take advantage of the spectrometer measurements by combining successive acquisitions of the slit spectral pixels to build a data cube. The reconstruction of the targeted regions, scanned by the spectrometer slit like a push broom remote sensing satellite, would be obtained by linearly interpolating the missing lines between every acquisition.

179

180



181

182

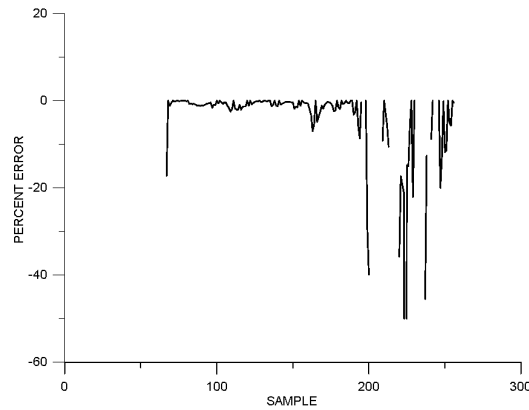
183

184

185

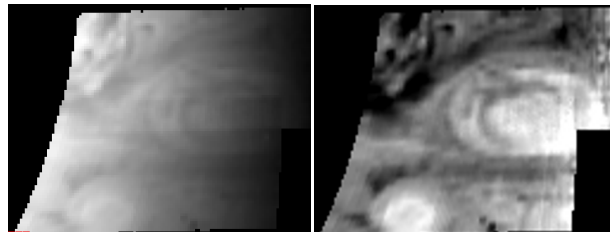
186

Figure 5 – As in Figure 3 but in relation to Figure 2b.



187
188
189
190
191
192
193

Figure 6 – As in Figure 4 but in relation to Figure 5.

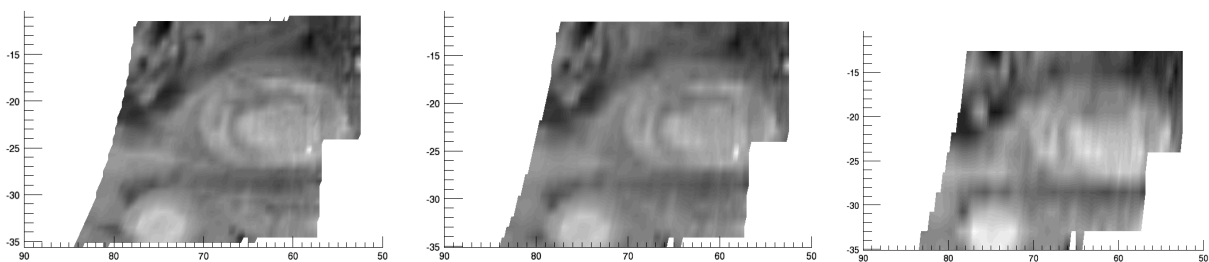


194
195
196
197
198

Figure 7 – The Jupiter Great Red Spot, as imaged by NIMS at 2 μm , before (a) and after (b) the Minnaert correction for the viewing and illumination angles.

199 A check of this method has been carried out on Jupiter spectral images acquired by NIMS during
200 the Galileo mission. Among the many NIMS observations, an image of the GRS (Great Red
201 Spot) is here reported as case study for its viewing geometry, alike to those of the incoming
202 JIRAM observations (Figure 7).

203



204

205 Figure 8 – The image of Figure 7 projected in System III planetocentric coordinates. In the three
206 panels we show the image obtained by removing 2 (a), 4 (b) and 8 (c) lines every one from the
207 original image, and linearly interpolating the surviving ones. This operation simulates the result
208 achievable from 0.06, 0.13 and 0.25 of degree separation, respectively, between the consecutive
209 slits of a future real observation of the JIRAM spectrometer.

210

211

212 The variations caused in the original image by viewing and illumination angle effects have been
 213 corrected by using a Minnaert function:

214

215

216

217

$$I(\mu, \mu_0) = I_0 \mu_0^k \mu^{k-1}$$

218 with μ the cosine of the emission angle (angle between the line of sight and normal to the
 219 surface) and μ_0 the cosine of the incidence angle (angle a solar ray makes with the normal to the
 220 surface) [7]. The Minnaert coefficient k has been determined from a fit to the data. From the
 221 resulting image different groups of lines have been removed to simulate different separation
 222 angles between each simulated scanning. In the NIMS case removing a line of pixels corresponds
 223 to give an interval of 0.5 mrad, corresponding to the IFOV, between two successive scanning. In
 224 Figure 8 the image reconstructions obtained by removing 2, 4 and 8 lines every one (equivalent
 225 to 0.06, 0.13 and 0.25 degree values of scanning interval) from the original image are shown.
 226 The outcomes of this case study suggest that a 0.13 deg value is a recommended choice as upper
 227 limit to recognize the principal features of an image. This finding has been a valuable input
 228 during the observations planning phase of the mission.

229

230

4. Conclusions

231 Some of the tools in preparation for the Juno/JIRAM data analysis have been described in this
 232 paper. The tool for the reconstruction of successive acquisitions of the spectrometer slit already
 233 demonstrated its utility in the observations planning phase. Future management of data mission
 234 will asks for always more refined processing tools. The work is in progress. Go Juno!

235

236

Acknowledgments

237 The JIRAM project for Juno is supported by the Italian Space Agency.

238

239

References

- 240 1. A. Adriani and the JIRAM Team, Space Science Reviews, doi:10.1007/s11214-014-0094-y
 241 (2014)
- 242 2. H. Becker *et al.*, Space Science Reviews, doi: 10.1007/s11214-017-0345-9 (2017).
- 243 3. D. Grassi *et al.*, Planetary and Space Science, doi:10.1016/j.pss.2010.05.003 (2010).
- 244 4. N. Divine. and H. B. Garrett, J. Geophys. Res.,88, 6889–6903 (1983).
- 245 5. H. B. Garrett *et al.*, JPL Publ., 03–006, 85 (2003).

- 246 6. H. B. Garrett *et al.*, *Geophys. Res. Letters*, 32, L04104 (2005).
- 247 7. H. C. Andrews and C. L. Patterson, *IEEE Transactions on ASSP*, 280, 26-53 (1976).
- 248 8. B. Hapke, *Icarus*, doi:10.1016/0019-1035(84)90054-X (1984).
- 249 9. C. A. Klein, *J. Appl. Phys.*, doi:10.1063/1.1656484 (1968).